

# Liquid crystalline spinning of spider silk

Fritz Vollrath\*† & David P. Knight\*

\* Zoology Department, University of Oxford, South Parks Road, Oxford OX1 3PS, UK

† Zoology Department, Universitetsparken B135, 8000 Aarhus C, Denmark

**Spider silk has outstanding mechanical properties despite being spun at close to ambient temperatures and pressures using water as the solvent. The spider achieves this feat of benign fibre processing by judiciously controlling the folding and crystallization of the main protein constituents, and by adding auxiliary compounds, to create a composite material of defined hierarchical structure. Because the 'spinning dope' (the material from which silk is spun) is liquid crystalline, spiders can draw it during extrusion into a hardened fibre using minimal forces. This process involves an unusual internal drawdown within the spider's spinneret that is not seen in industrial fibre processing, followed by a conventional external drawdown after the dope has left the spinneret. Successful copying of the spider's internal processing and precise control over protein folding, combined with knowledge of the gene sequences of its spinning dopes, could permit industrial production of silk-based fibres with unique properties under benign conditions.**

**F**abric fashioned of threads reeled from cocoons of the silkworm have long been one of the mainstays of world commerce, until the demands and constraints of the Second World War helped man-made fibres derived from petrochemical raw materials, or feedstocks, to supercede silk. Today, millions of tons of nylon are produced each year, selling for 2–10 US dollars per kilogram<sup>1</sup>, whereas world silk production reaches only about 70,000 ton per year, with quality fibres selling for about 40 US dollars per kilogram. The current production rate and price of silk (<http://www.kanex.or.jp/groups/home/MARKET/XKitChart.htm>) are thus similar to that of top quality man-made fibres such as Kevlar and Twaron. However, silk polymers are poised for a possible comeback, albeit with a twist: artificial fibres spun from dope solutions composed of genetically modified (GM) natural proteins, designer proteins or protein–plastic blends<sup>2–5</sup> could be the new 'techno-silks'.

Parent silk gene-motifs to create GM feedstocks for artificial dope solutions are likely to be taken from the golden silk spider *Nephila clavipes*, rather than from the moth *Bombyx mori*<sup>6</sup>, which has classically been the main silk provider. This preference is largely because spider silk is much tougher than the stiff but brittle cocoon threads of the moth, reflecting the fact that spider threads have evolved to arrest 'aerial missiles' rather than form a protective cradle. After all, silk has been an arachnid construction material for about 400 million years<sup>7</sup>, of which half has seen web-engineering responding to the demanding specifications of an aerial arms race with jumping and flying prey<sup>8</sup>. Accordingly, advanced web spiders have evolved an armory of highly specialized silks. (See Box 1b for an illustration of the range of mechanical properties of silks produced by different web spiders).

Spider dragline silks, the main structural web silk, which are also used for the spider's lifeline, are exceptionally strong and extensible<sup>6</sup>, making them very tough fibres. Indeed, their toughness equals that of commercial polyaramid (aromatic nylon) filaments, which themselves are benchmarks of modern polymer fibre technology. Polyaramids are used to make materials ranging from radial tyres and bulletproof clothing to reinforced composites for aircraft panels. The exceptional toughness of dragline silk is achieved under benign conditions: in contrast to current technopolymers based on petrochemicals, the spider spins its totally recyclable fibres at ambient temperatures, low pressures and with water as solvent<sup>9,10</sup>. There are accordingly many advantages to copying the spider's silk and silk production capabilities<sup>11</sup>: genetically engineered silk with specially tailored properties and spun using 'green' processes could replace the ubiquitous plastics, which are often detrimental to the environment in both production and

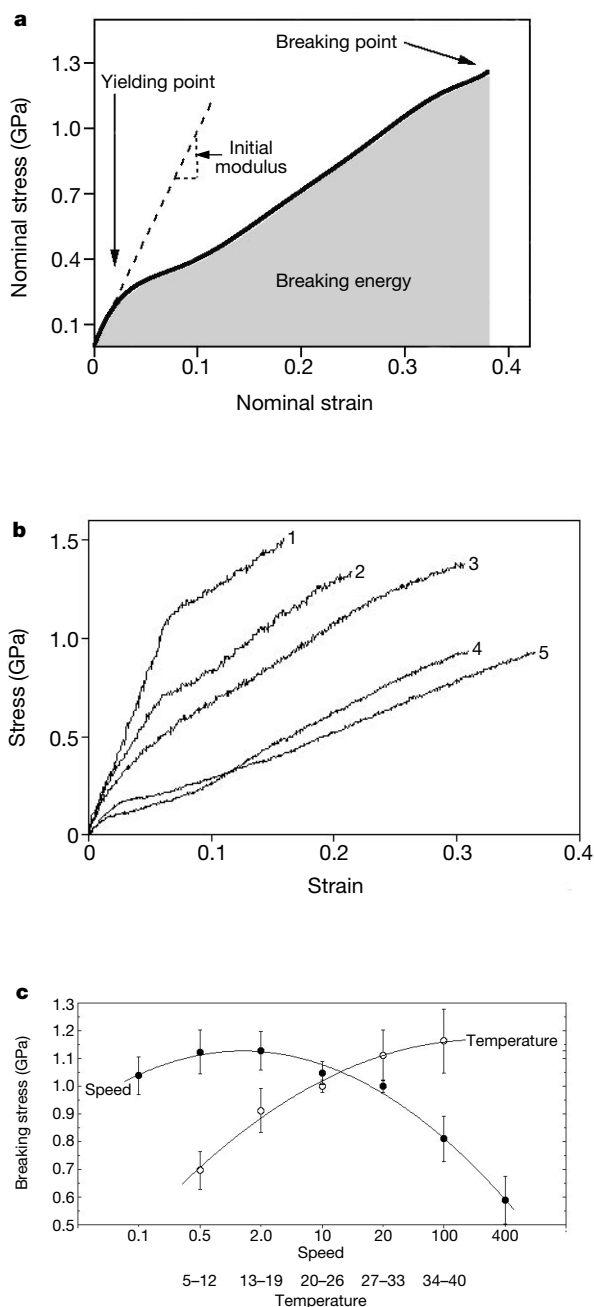
disposal<sup>13</sup>. In fact, spider silk has already been spun artificially: the most interesting methods until now include conventional solvent spinning of recombinant spider silk protein analogue by Du Pont Ltd<sup>2</sup> and extruding regenerated silk into a coagulation bath using a nanofabricated silicon spinneret<sup>12</sup>. The race is now on to perfect spinning technology<sup>13</sup>. Of course, artificial silk could be a potential economic threat to rural producers of natural silks, but the overall benefits might still outweigh the costs and disadvantages, especially if the dope-feedstock used for the production of these techno-silks is derived from agricultural products, such as goat milk genetically modified to contain spidroins, the major proteins of spider dragline silk (see <http://www.nexiabiotech.com>).

To mimic spider dragline silk successfully we must copy the crucial design features of both the feedstock dope proteins and the spinning process. Molecular biology provides the potential to extract, synthesize and assemble artificial genes to supply feedstocks for the production of silks<sup>14–16</sup>, whereas classical morphological studies provide construction details of the spider's extrusion system<sup>17–21</sup>. Together, these two biological disciplines can lead to the design of first prototypes for a highly advanced and benign fibre extrusion technology, and close collaboration with process engineering should eventually allow commercialization. Scientifically as well as technologically, achieving this goal would be an innovation. It would be the first time that a whole natural production system as complex as the spider's has been copied in totality from gene to marketable product, though there are many examples of industry copying an aspect of nature, including Velcro which mimics the way seed hooks snag in fur.

## Composition of a thread

Spider and insect silks have the same basic building blocks: proteins made largely from non-essential amino acids<sup>22,23</sup>. Although they evolved independently in a wide range of invertebrates<sup>24</sup>, all but the faecal fibres of beetles are extrusions of specialist silk glands (Box 2). Insects have found many ways of making a wide range of silk types, but web spiders are unique in maintaining, in the same individual, a battery of highly specialized glands producing very different silks, often simultaneously<sup>25</sup> (Fig. 1). This diversity is driven by the central role played by silk in a spider's life and by the tight co-evolution of silk and behaviour such as prey capture, shelter construction and reproduction<sup>26</sup>. Although the different silk glands in an advanced web spider like *Nephila* are likely to have evolved from a single type of gland, they now differ significantly from one another in morphology, anatomy and composition<sup>27</sup> to allow for the production of different silks (Fig. 1). Moreover, there seems to be significant variability in silk properties even for the same silk produced by

Box 1  
Stronger than steel



Silk, like many man-made fibres, is viscoelastic<sup>73</sup>; loading and unloading paths are not the same as they would be in a perfectly elastic material. Moreover, a small plastic component is also often observed (that is, the material does not recover fully to its original length upon relaxation), but this can be overcome by curing with water<sup>74</sup>. The mechanical properties of a fibre are best described by the shape of a response curve when the material is stretched (**a**). Such stress–strain curves may vary greatly between the same type of silk from different spiders (**b**) and typically vary between the different silks from the same spider<sup>26</sup>. The variability is due to differences in both the chemical composition of the dope and the conditions under which it is spun, once again emphasizing the importance of the spinning environment to control the material properties of the final silk thread (**c**). The spider

can easily vary spinning conditions by adjusting running speed, or changing speed of pulling silk with the legs (if used) and, finally, by building its webs during different times of the day or night (which affects temperature) all of which gives the animal some degree of control over the performance of the thread it produces.

Spider silk is light as well as strong. Its strength of 1.1 GPa approaches that of typical high tensile engineering steel (1.3 GPa), but silks have a significantly lower relative density (1.3) than steel (7.8) (ref. 73). Compared on a weight basis, silk is thus by far the stronger material. To probe the mechanical behaviour of silk (**c**), we stretch our silk at a specific rate  $dl/dt$  and measure the force  $F$  required to cause a given extension  $dl$ . We generally consider the engineering stress ( $\sigma_E$ ), which is the force applied to the cross-sectional area ( $A_0$ ) of the sample, to be constant during the test, even though  $A_0$  will decrease somewhat during stretching. The normalized engineering strain of extension ( $\epsilon_E$ ) is the ratio of change in length ( $dl$ ) to the initial gauge length ( $l_0$ ). The ratio of stress to strain, given as Young's modulus ( $E$ ) and derived from the slope of the curve, is a measure of the fibre's stiffness. Typically there is at least one 'yield point', that is, a point at which the curve suddenly changes slope because of major structural transitions in the material. The area under the curve (if the fibre breaks) or between hysteresis curves (if the fibre is relaxed before it breaks) indicates the fibre's toughness, and thus the energy taken up by the material (**a**). **a**, Typical stress–strain curve for spider dragline silk reeled from a *Nephila edulis* female, based on experimental data. The data are obtained from stretching experiments on dragline silk, giving the force (stress) required to reach a given strain, with strain indicating the fibre's extension under stress relative to its extension in the relaxed state. Average data (mean  $\pm$  standard deviation, s.d.) for silk collected at  $20 \text{ mm s}^{-1}$  and  $25^\circ\text{C}$  from an adult *Nephila edulis* female are: silk diameter,  $3.35 \pm 0.63 \mu\text{m}$ , tensile breaking strain,  $0.39 \pm 0.08$ ; breaking stress,  $1.15 \pm 0.20 \text{ GPa}$ ; initial modulus,  $7.9 \pm 1.8 \text{ GPa}$ ; yield stress,  $0.15 \pm 0.06 \text{ GPa}$ ; and breaking energy,  $165 \pm 30 \text{ kJ kg}^{-1}$  (after ref. 63). Comparable data for Kevlar 81 high tenacity yarn 98 are: diameter,  $12 \mu\text{m}$ ; breaking strain 0.05; breaking stress 3.6 GPa; modulus 90 GPa; no yield stress as yarn has a single modulus; and breaking energy around  $33 \text{ kJ kg}^{-1}$  (A. Grandus, personal communication). Thus Kevlar is 3 times stronger but spider silk is 5 times tougher because it is 8 times more extendible. **b**, Stress–strain characteristics of dragline silk reeled from different web building spiders: *Euprostheno* sp (Pisauridae) (**1**), *Cyrtophora citricola* (Araneidae) (**2**), *Latrodectus mactans* (Theridiidae) (**3**), *Araneus diadematus* (Araneidae) (**4**) and *Nephila edulis* (Tetragnathidae) (**5**). The data (modified from ref. 28) were collected under comparable conditions by artificial reeling. They show that the silk of *Euprostheno* (**1**) is stiffer and requires more force to break it but is much less elastic and thus takes up less energy than the comparable silk of *Nephila* (**5**); the characteristics of the other species lie in between. We note also the differences in the initial moduli and yielding points. **c**, The effect of spinning conditions on the breaking stress of dragline silk spun by *Nephila edulis*. The black circles give the effects of modifying reeling speed (in  $\text{mm s}^{-1}$ ) and the white circles those of modifying body temperature (in  $^\circ\text{C}$ ) (figure from ref. 63). The average breaking energy for the sample threads at control conditions was  $165 \pm 30 \text{ kJ kg}^{-1}$  (ref. 63). In the graph, breaking stress is used rather than breaking force because the differences between individual spiders (as well as silk reeling speed and body temperature) affect the diameter of the silk thread, which in turn influences the force needed to break the thread (see ref. 63). The control temperature was  $25^\circ\text{C}$  when the reeling speed was varied, and the control speed was set to  $20 \text{ mm s}^{-1}$  when the body temperature was varied<sup>63</sup>, with the average natural spinning conditions for this species taken to match the control conditions<sup>63</sup>. (Each data point derives from threads of 4–11 spiders with four pieces of each thread measured, mean  $\pm$  s.d.; figure modified from ref. 63.)

the same spider on different days, or even on the same day under different environmental conditions<sup>28</sup>. Most of these differences are attributable to varying spinning conditions, but they may also reflect considerable variability in the amino acid composition of the spinning dope produced by a gland<sup>22,23,29</sup>, some of which might be affected by diet<sup>29,30</sup>.

Gene sequences are being mapped for rapidly increasing numbers of silks<sup>15,16,31–34</sup> and first-generation models are beginning to relate protein structure to the mechanical properties of the thread<sup>35,36</sup> (see Box 3). But although gene sequences can predict average domain sizes along the protein backbone, any deeper understanding of the mechanical properties of spider silk requires additional information on the interaction between the different proteins in a thread and the full structure at all hierarchical levels. And even though spider silk seems a poor cousin in terms of diversity, with only two or three spider silk protein gene families identified so far<sup>15,16,33</sup> (a large number of different proteins, corresponding to many genes, have been identified in the silks of some chironomid midges<sup>37</sup>), shunting and splicing would allow a spider to create a wealth of spider silk proteins from quite a parsimonious genetic blueprint<sup>29–31</sup>. More-

over, expression differences in each of the spider's seven different gland types allow transcriptional regulation to produce a wide variety of gland-specific silks with different compositions and material properties<sup>16</sup>.

At least one spider silk protein family (found, for example, in the golden silk spider *Nephila clavipes* and the garden cross-spider *Araneus diadematus*) encodes for polypeptides that contain a variable number of both crystalline poly-alanine domains as well as less-crystalline glycine-rich domains<sup>15,16,32,97</sup>. Although there is consensus that silk contains crystalline and non-crystalline regions, the structure of the glycine-rich regions is imperfectly understood. Indeed, the classic concept of dragline silk being comprised of  $\beta$ -sheet crystals packed in a rubbery matrix of random-coiled springs<sup>35,36,38</sup> has been challenged<sup>39,40</sup> following the observation that silk may contain a range of conformations such as 'random coil',  $\beta$ -turns and parallel and/or antiparallel  $\beta$ -pleated sheet crystals,  $\alpha$ -helices or the more compact and left-handed 3(1)-helices<sup>35,36,38–40</sup> (see Box 3 for further details). Clearly, before we can copy silk to full effect we must determine the secondary structure of polypeptide chain folding as well as higher-order structures of the protein constituents. For example, recent studies have shown that a single spider silk filament can have a complex 'coat-skin-core' organization<sup>41,42</sup> with micro-fibrils<sup>43–45</sup> enclosing fine channels<sup>41</sup> that might impart energy-dispersive properties<sup>46</sup> by deflecting the tips of cracks forcing their way across the thread. Because this structural complexity is likely to contribute significantly to the toughness of spider silk, it must be taken into account when attempting to design and spin biomimetic silks.

## Box 2

### Other spinning arthropods

*Bombyx mori* is a domesticated moth with a larva that feeds on mulberry leaves. Its pupation cocoon is unravelled to give the classic commercial silk; other commercial silks come from other moths, such as *Antheraea*. Our knowledge of the spinning processes in these insects is extensive but incomplete<sup>48,75</sup>. The paired silk glands are long and heavily tracheated ectodermal ducts that open on the lips of the mouth. Silk fibroin and droplets, which later form canaliculi, are secreted at the posterior end of the gland and move along in laminar flow while being coated by three layers of sericin, the silk's second protein constituent<sup>76,77</sup>. The first, thin coating contains one polypeptide (s-4), the second, thicker granular layer contains two (s-1 and s-3) and the thin, third layer contains a further two polypeptides (s-2 and s-5)<sup>48,77</sup>. All these polypeptides are rich in glycine, serine and aspartic acid, and s-1 and s-2 also contain sugars<sup>77</sup>. Thus coated, the silk filament is drawn (the larva pulls by moving its head) through a cuticle-lined duct to join its companion filament made in the other branch of the bilaterally symmetrical silk organ. Both filaments are then glued together by secretions from Filippi's gland, with the still pliable sericin being moulded by the silk press (a muscular valve) and the labial opening<sup>75,77</sup>. A silkworm silk gland thus consists of a posterior part producing silk-dope, three distinct middle parts producing sericin-coat, a tapering duct, a Y-junction joining the two glands, followed by a single press and opening. In a cocooning *Bombyx* larva, this organ constitutes about 20% of the animal's body weight, and a single cocoon will yield about 800 m of silk fibre composed of two filaments, each with an average diameter of about 10  $\mu\text{m}$  (ref. 75). The heavily coated fibres are stiff and strong, but not very tough because they lack extensibility. Silk production is not confined to moths and spiders<sup>24</sup>: bees and wasps (Hymenoptera) embed simple silk fibres into the wax of their combs to provide strength<sup>78</sup>, fleas (Siphonaptera) use silk in their nests and cocoons<sup>79</sup>, lacewings (Neuroptera) employ it to cement eggs onto stalks<sup>80</sup>, caddisfly larvae (Trichoptera) use it to bind debris into houses or make underwater webs<sup>81</sup>, aquatic midge larvae (Diptera) use it to construct feeding nets and tubes for housing and pupation<sup>37</sup> and glow worms (Coleoptera) and fungus gnats (Nematocera) make sticky silk lines to catch flies<sup>82</sup>. Among the arachnids, silk is used for nest building in the pseudoscorpions and mites<sup>83</sup>, and in all aspects of life in the true spiders (Araneids)<sup>19</sup>. Diversity in taxonomy, modes of deployment and evolutionary pathways resulted in a wide range of molecular chemistries, material properties and spinning technologies<sup>24</sup> associated with silk production, thus providing ample scope for biomimetic material design and processing.

### Spinning a fibre

Let us take the production of dragline silk by *Nephila* as an example of a spider's advanced spinning technology, given that the process is best understood in this species and probably representative for dragline spinning by all orb-spiders. Figure 2 gives a schematic illustration of the different components of the spinning duct, the structure through which the spider extrudes its silk and which is analogous to the 'die' used in artificial fibre spinning technology. The major ampullate gland making this silk consists of a long tail and a wider sac. The tail secretes the major part of the so-called 'spinning dope', a solution containing the protein molecules used to make the silk fibre dissolved in water, while the sac constitutes the main storage repository that leads, through a 'funnel', to a tapering duct. Much of the fibre formation occurs in this duct, which has three loops inside a sheath and terminates in a structure known as the valve. After the valve, further processing proceeds in a narrow tubular region specialized for rapid water recovery, and the silk thread then exits at the spigot whose flexible lips fit tightly round the silk thread, a feature assumed to assist in water retention<sup>21</sup>. Tail and sac of the gland are about 60 mm in length and, when full, weigh in at about 10 mg the pair, about 1% of the total bodyweight of a lean adult female (D.P.K. and F.V., unpublished work).

The secretory part of the gland has two distinct transverse zones, the A-zone occupying the tail and first part of the sac, and the B-zone running from the widest part of the sac to the funnel. The epithelium of the A-zone is composed of tall columnar secretory cells of a single type, packed with secretory granules (see Fig. 2, inset A). The output of these cells is an aqueous and highly viscous, often yellow solution of about 50% protein<sup>47</sup>, which will be mostly spidroin I and II, the main proteins making up spider dragline silk<sup>2</sup>. The solution secreted by the A-zone is not a homogeneous liquid, but contains many small spherical droplets comparable to those found in silkworm silk dope<sup>48</sup>. These droplets flow along the tail and sac<sup>49</sup> in the spidroin matrix, and are thought to first grow by coalescence before being drawn out into long thin structures, the canaliculi<sup>41,49</sup>. As the A-zone secretion flows towards the funnel it is coated by a colourless homogeneous viscous liquid secreted in the B-zone. Although the cells of the B-zone superficially resemble

those of the A-zone (see Fig. 2, inset B), they contain different secretory granules, many of them filled with a hexagonal columnar liquid crystalline material. Given the relative size and locations of these zones, we may assume that the more extensive A-zone (about 75% of the epithelium) secretes the spidroin(s), whereas the smaller B-zone in orb-web spiders secretes coat protein(s), possibly the glycoprotein identified histochemically in the gland<sup>17</sup> and biochemically in the thread<sup>50</sup>. The glycoprotein may help to plasticize the thread by maintaining a high water content<sup>51</sup>.

Within the major ampullate gland and the first and second loop, or limb, of the spinning duct, the spider's dope<sup>49,52,53</sup>, like the silkworm's<sup>54,55</sup>, is liquid crystalline, with the main silk protein constituent likely to be in a compact conformation that allows it to be processed at high concentrations<sup>47</sup>. Liquid crystallinity offers desirable properties, which make it possible to efficiently spin a thread from molecules as large as silk proteins (see Box 4). Specifically, in the spider's gland and duct the molecules seem to form a nematic phase<sup>49</sup>, that is, they form a substance that flows as a liquid but maintains some of the orientational order characteristic of a crystal, with the long axes of neighbouring molecules aligned

approximately parallel to one another. Liquid crystallinity would thus allow the viscous silk protein solution to flow slowly through the storage sac and duct while the molecules form complex alignment patterns. In the spider's gland, the long axes of the rod-shaped silk protein molecules or molecular aggregates appear<sup>49</sup> to be oriented perpendicular to the secreting epithelium walls when close to them, but gradually bend over with increasing distance until—along the midline of the glandular sac—they lie parallel to the long axis. This arrangement (called a simple escaped nematic texture) persists from the gland into the first limb of the duct, but changes into a more complex escaped nematic texture in the second limb of the duct, where the narrower lumen forces the molecules to bend forwards and backwards in an alternating pattern known as the cellular optical texture<sup>49,56</sup>. This arrangement is commonly seen when 'nematic discotic' liquid crystals are confined in narrow tubes<sup>56</sup>. This type of liquid crystal forms bilayered disks in which the rod-shaped molecules are arranged perpendicular to the plane of the disk<sup>56</sup>. It seems likely that the perpendicular arrangement of the silk protein molecules at the secreting epithelium walls and the subsequent nematic escape into an arrangement that is parallel to

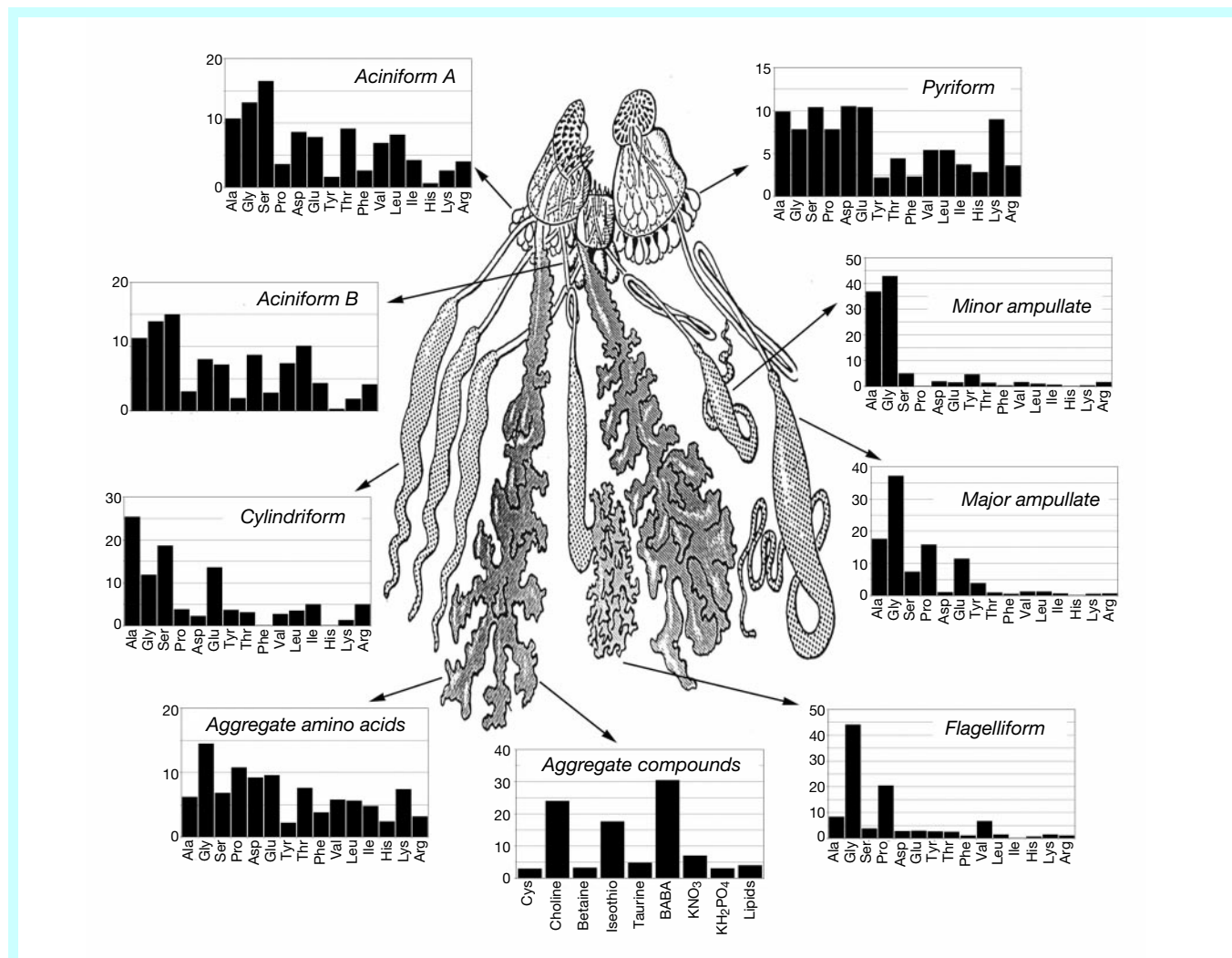


**Figure 1** The seven specialized glands and their different amino acid compositions of a typical Araneid orb weaver. Silk glands are paired, reflecting their evolution from limb glands<sup>64</sup>. The aciniform glands make the silk for wrapping prey, the cylindriform glands make the cover silk for the egg sac and the pyriform glands make the silk for attachments and for joining threads<sup>25,27</sup>. The major and minor ampullate glands are of similar shape; the major glands provide the silk for the spider's dragline and the frame threads of its web while the minor ones provide threads that can be added to any structural thread and may be used for the radial (spoke) threads of the web<sup>25,27</sup>. The flagelliform glands provide the core of the threads of the capture spiral, while the threads' coating is supplied by the aggregate glands. This coating contains glycoproteins for stickiness<sup>65</sup>, salts to act as bactericides<sup>66</sup> and hygroscopic organic compounds<sup>67</sup> that, in addition to being bactericidal, also attract atmospheric water<sup>68</sup> to plasticize the core of the thread<sup>69</sup>. (Glands after ref. 70 and amino acid compositions after ref. 22; we note there can be variability in composition within each gland, which may be adaptive<sup>29</sup>).

the long axis of the silk gland and spinning duct prevent the liquid crystalline dope from breaking up into numerous small domains. This in turn would suppress the formation of disclinations, a form of defect somewhat analogous to dislocations in solid crystals and which are likely to diminish the tensile strength of the spun thread<sup>49,57</sup>.

The duct's convergent, or hyperbolic, geometry forces the dope flowing along it to elongate at a practically constant rate<sup>49</sup>. As a result, the spherical droplets in the dope extend to form the long, thin and axially orientated canaliculi<sup>21,49</sup>, which are thought to contribute to the thread's toughness<sup>46</sup>. The slow, constant nature of the elongation also ensures that only low and uniform stresses are generated. This prevents localized coagulation centres from forming prematurely<sup>49</sup>, that is before the silk protein molecules in the dope have reached their optimal orientation. As in any other spinning, good molecular alignment contributes significantly to the thread's toughness<sup>2,3,57,58</sup>.

A much higher stress is likely to be generated during rapid extension in what we have called the "internal drawdown taper"<sup>21</sup> (see Fig. 2, panel X). This starts where the forming thread suddenly stretches, narrows and pulls away from the walls of the third limb of the duct (in the fully grown spider approximately 4 mm before the exit spigot)<sup>21,49</sup> (see below). The high stress forces generated during this stage of processing probably bring the dope molecules into alignment and into a more extended conformation, so that they are able to join together with hydrogen bonds like zip fasteners to give the anti-parallel beta conformation of the final thread. As the silk protein molecules aggregate and crystallize, they will become more hydrophobic, which should induce phase separation and hence the loss of water from the surface of the solidifying thread. Recent studies of the flow behaviour of dope solutions *in vitro* (Chen, X.,

D.P.K and F.V., unpublished work) and the observation that the force needed to reel silk *in vivo* increases with reeling speed<sup>59</sup> (except at very high reeling speeds) provides direct evidence that such a stress-induced phase separation does indeed occur. The secretion of hydrogen ions, by proton pumps located in the epithelial cells of the third limb of the duct, renders the dope solution more acidic, which should assist phase separation<sup>20,59</sup>. The concluding drawdown of the silk, to produce the final fibre, occurs in the air after the thread has left the spigot<sup>21,60</sup> and is probably accompanied by further loss of water by evaporation<sup>53,60</sup>. However, as some natural silks are successfully spun underwater<sup>37</sup>, water loss by evaporation is not always necessary.

The spider's simultaneous and internal drawdown and material processing which exploits phase-separation differs dramatically from that used in industrial spinning, where the solvent escapes in a gradient or to the surface, typically at the die's external opening<sup>57</sup>. Although the latter type of processing, with external drawdown into air, may occur in the spinning glands of other spiders<sup>61</sup>, keeping the drawing process inside the animal appears to offer conspicuous advantages: most of the water from the dope can be recycled by absorption from the distal part of the duct<sup>62</sup>, and the duct acts as a combined internal die and a treatment and coating bath<sup>20</sup>.

As the fibre forms from the dope, it pulls away from the surrounding walls of the spinneret. This initial phase of the drawdown should start at that location in the duct where the force required for drawing out a thread by extensional flow balances or just falls beneath the force required for moving along the liquid dope in contact with the walls. As it moves through the spinneret, the forming thread is probably mostly lubricated by water formed in the phase separation. A surfactant secreted into the third limb of the

### Box 3

#### Silk proteins and genes

Spider silk proteins are only partially characterized, even for *Nephila clavipes*<sup>64</sup>, the spider species that has been most studied and which is thus our benchmark. Separating the proteins by sodium dodecyl sulphate–polyacrylamide gel electrophoresis suggests that the major ampullate gland in this species secretes a single major protein component, whose apparent molecular weight has been determined as 275 kDa (ref. 85) and 320 kDa (ref. 86). The parent protein is about 5% glycosylated<sup>60</sup> and seems to contain sequences derived from Spidroin I and one or more additional domains not seen in either Spidroin I or II (ref. 85). Initial characterizations suggest that the protein is constructed from two peptide chains held together by 3–5 disulphide bonds<sup>85</sup>, which may aggregate under native conditions to give an oligomer with a molecular weight of about 725 kDa (ref. 2). Another component, with an estimated molecular weight of 180 kDa, has been identified in mercaptoethanol-reduced silk<sup>85</sup>. Until now, only a few silk genes have been partially sequenced, and most of these are from orb spiders<sup>64</sup>. Spidroin I and Spidroin II are two subunits of dragline silk found in the major ampullate glands<sup>64</sup>. A very different protein, containing only three motifs repeated many times in the same order, is secreted by the flagelliform glands<sup>31</sup>; it forms a major component of the elastic support fibre of the capture spiral of the spider's web. The largest of the protein's three motifs, (Gly-Pro-Gly-Gly-X)<sub>n</sub>, may form a β-spiral or helix composed of a large number of β-turns arranged end-to-end; these can then act as springs, which bond together via water bridges at the X-residues to form a highly elastic network<sup>81</sup>. In contrast, the sequence data for Spidroin I and II show an alternation of hydrophobic polyalanine domains and less hydrophobic glycine-rich domains. If we are to understand the way in which the protein refolds during spinning, we need to clarify its structure during production and storage in the gland cells and sac. Spidroin may form rod-shaped molecular or supramolecular units, which can be stored as a highly concentrated liquid crystalline solution to form a fibre when

strained in the spinning duct<sup>49</sup>. It seems that unspun spidroin differs in conformation from the silk thread, but resembles silk-I of silkworm dope<sup>47</sup>. NMR and ultraviolet circular dichroism<sup>47</sup> measurements on unspun spider dope indicate that it lacks the β-pleat seen in the final silk and instead contains up to about 30% α-helices, 40% of a 'random coil' conformation, and 30% β-turns that might exist in a loose and dynamic, partially extended configuration analogous to that of the molten globule state. Taken together, the observational evidence suggests a multiple β-turn structure for the unspun dope; this might contain triple<sup>87</sup> or double<sup>88</sup> β-turns stabilized by interstrand hydrogen bonds, or a β-turn/'random coil'/α-helical structure<sup>47</sup>. The location of the β-turns and α-helix motifs is not known with certainty, but in aqueous solution, the glycine-rich regions and the polyalanine sequence are likely to form the β-turns and α-helices, respectively<sup>84</sup>. Advanced imaging techniques such as NMR, micro-Raman spectroscopy and micro-X-ray diffraction are crucial for analysing the structure of the secondary and tertiary conformations of the silk dope and thread. For example, proton-driven <sup>13</sup>C two-dimensional NMR spin-diffusion experiments on *Nephila* dragline silk thread suggest that the poly-Ala segments adopt a highly ordered β-sheet structure<sup>39,47</sup> and the glycine-rich segments 3(1) helical structures<sup>40,88</sup>, both oriented in line with the thread. Raman spectroscopy on single *Bombyx* and *Nephila* threads during progressive stressing shows that the silk microstructure experiences uniform stress during deformation in both spider and silkworm silk<sup>89–91</sup>, suggesting the presence of microfibrillar structures inside the thread that would evenly distribute any applied stress. X-ray diffraction patterns obtained from single threads being spun<sup>92</sup> also reveal that the thread consists of small crystalline blocks in a matrix containing both oriented and disoriented amorphous material, with the crystalline fraction having a β-poly (L-alanine) structure<sup>93</sup>.

duct may also help to reduce the force required for drawdown. The tapered nature of the duct may allow the point of drawdown to move along the duct according to the rate of spinning, thus resulting in thread diameters adjusted to the speed of spinning<sup>63</sup>.

In summary, spiders make exquisite use of internal spinning of liquid crystalline dope in an acid bath, followed by further drawdown in the external air gap, to produce silk threads of high toughness and elasticity. Spinning of liquid crystalline material, as

done by spiders, has several advantages: (1) it is virtually free of the uncontrolled reorientation of molecules after emergence from the die; (2) the force required to spin a thread is small; and (3) pre-alignment of the molecules in the unspun dope may reduce the formation of defects<sup>57</sup>. It seems that much stands to be gained by trying to understand and copy the spinning technology, which the spider has evolved over millions of years to regulate the folding and refolding of macromolecules under highly controlled conditions to

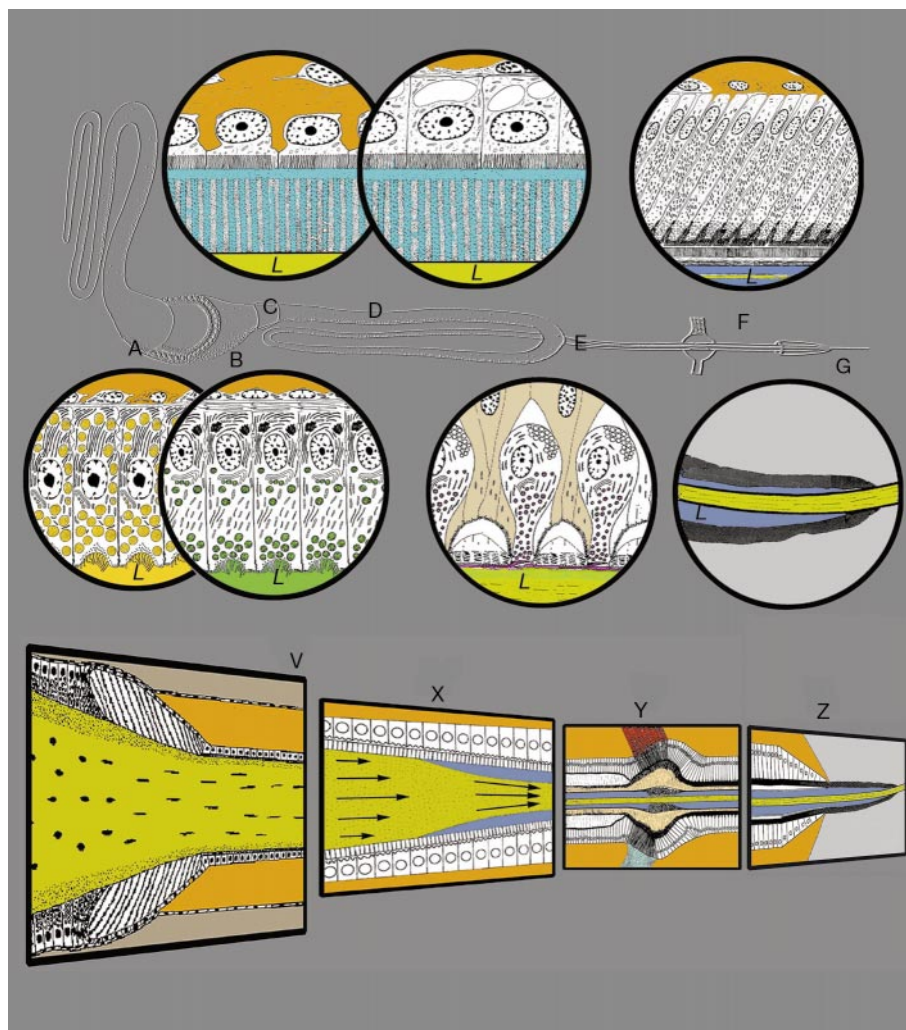


**Figure 2** A spider's dragline spinneret. The top part shows original drawings of the histology of the spinneret (lumen, L); the bottom part outlines its spinning function, which entails drawing the liquid crystalline dope solution produced in the gland through a tapering s-shaped duct, thereby converting it into an elastic thread. Dope production occurs in two zones: the A-zone of the gland (see panel A) secretes spidroin, the protein forming the core of the thread, while the B-zone (see panel B) secretes the thread's thin coat. The secretory vesicles of the A-zone contain short, narrow filaments; most of those of the B-zone contain hexagonal columnar liquid crystals. The greatly thickened cuticle of the funnel (clearly visible in panel V) anchors the extensible duct to the less mobile sac, perhaps to prevent shearing of the dope when the spider wiggles. The duct itself has a thin cuticle, which acts as a dialysis membrane and may allow water<sup>20</sup> and sodium ions out of the lumen, and potassium ions<sup>71</sup>, surfactants and lubricants into the lumen to facilitate thread formation (see panel X). The epithelium of the s-shaped duct progressively increases in height from the funnel to the valve, suggesting increased pumping of water and ions as the dope is drawn through the duct (panels C and D show the histology of epithelium in the first and second limbs, respectively). The drawdown process is mainly internal and starts in the third limb of the duct (see panel X), approximately 4 mm from the exit spigot. Just before and after the start of the drawdown taper, single flask-shaped gland cells, such as seen in inset E, may contribute an extra coating to the thread<sup>21</sup>. The 'valve', shown in panel Y in the bottom of the figure, is not a restriction nozzle, but a clamp for gripping the thread<sup>21</sup>. It may also act as a 'ratchet' or 'pump', to restart spinning after internal rupture of a filament<sup>21</sup>. The section of duct (see inset F) after the valve appears to be highly specialized for water pumping, having tall cells with numerous mitochondria and apical microvilli and a large surface area provided by apical infoldings of the plasma membrane<sup>20</sup>. Finally, the thread is gripped by the flexible and elastic lips of the spigot (inset G), through which it passes to the outside world (see panel Z). The spigot strips off the last of the aqueous phase surrounding the thread, thus helping to retain water in the spider, and also places the thread under tension for the final air-drawing step<sup>21,60</sup>. The diameters of the round panels are A: 93  $\mu\text{m}$ , B 93  $\mu\text{m}$ , C 12  $\mu\text{m}$ , D 12  $\mu\text{m}$ , E 70  $\mu\text{m}$ , F 288  $\mu\text{m}$ , G 60  $\mu\text{m}$  (drawings based on light microscopy, SEM, CryoSEM energy dispersive X-ray analysis and TEM studies of the major ampullate gland of three species of *Nephila*); the heights at midpoint of the frame panels are V (funnel) 350  $\mu\text{m}$ , X (drawdown) 40  $\mu\text{m}$ , Y (valve) 300  $\mu\text{m}$ , Z (spigot) 190  $\mu\text{m}$ .

## Box 4

## Liquid crystalline spinning

The rheology of liquid crystalline solutions is non-newtonian and differs from that of isotropic solutions, a feature that can be exploited by a biological system under intense pressure to adapt and optimize. In particular, while liquid crystalline viscosity depends on the shear rate, stress forces along and across the flow lines of the liquid are highly dependent on the concentration of the solution and can be very small indeed<sup>57,58</sup>. By controlling the solvent saturation (that is, the water content) of the liquid crystalline spinning solution, the spider can thus vastly reduce its metabolic cost of silk production and use narrow extrusion ducts — which would otherwise require high energy input to operate — to produce very fine fibres ranging from a few nanometres to a few micrometres in diameter<sup>57,94</sup>. Newtonian laminar flow (where the shear rate determines the stress forces but not the viscosity), in contrast, is characterized by a nonlinear relationship between the coefficient of flow viscosity,  $h_t$ , and the tube radius,  $R$ , (that is,  $h_t = \rho R^4/8Q \cdot dp/dl \cdot h_0$ ), as well as the speed of spinning (through  $Q$ , the volume rate of flow, and  $dp/dl$ , the gradient of the pressure  $p$  along the tube length  $l$ )<sup>94</sup>. Clearly, making fibres under newtonian conditions would require very high pulling forces that could not be generated by a spider walking<sup>25</sup> either at normal speed (20 mm s<sup>-1</sup>) or rushing at 800 mm s<sup>-1</sup>. Moreover, in newtonian flow, viscosity increases with decreasing temperature:  $h_t = h_0 \exp(E_a/RT)$ , where  $h_0$  is the basic viscosity and  $E_a$  the activation energy, which depends on the molecular structure of the polymer<sup>95</sup>. The relative temperature independence of non-newtonian flow, in contrast, would benefit a spider by allowing it to spin webs in the cold early hours of the morning as easily as in the heat of noon. Both spider and moth have found ways to employ non-newtonian fluid dynamics in order to make thin silk filaments at ambient temperatures and low energy costs, by using liquid crystallinity, well adjusted protein concentrations and reasonably low spinning speeds (and hence shear rates). Shear thinning, a decrease in viscosity resulting from moderate increases in shear rate has been observed in nematic liquid polymers and also in spider silk dope solutions (Chen, X., D.P.K. and F.V., unpublished work); it will further help to reduce the energy required to flow the dope through the spider's spinning duct. Although liquid crystalline polymers behave as newtonian fluids at high dilutions, at high concentrations their flow is non-newtonian (that is, viscosity depends on strain rate and strain history) and the apparent viscosity at first increases with concentration but then actually decreases to initially low levels<sup>58</sup>. This is because the molecules tend to align at high concentrations, enabling them to slide or roll past each other more easily<sup>57</sup>. Rod-like liquid crystalline molecules with length  $L$  in solutions (of concentrations  $c$ ) diluted to  $c \ll 1/L^3$  have a viscosity

$h = h_s(1 + cL^3)$ , which is practically that of the solvent; in solutions where  $c \gg 1/L^3$ , the viscosity greatly increases to  $h = h_s(1 + (cL^3)^3)$ , and is thus much more dependent on molecular length and therefore on molecular weight<sup>57</sup>. Liquid crystalline viscosity is strongly affected by the vibrational freedom of the molecules, making it very sensitive to both the rate and history of shear and thus leading to strong non-newtonian viscoelasticity<sup>57</sup>. Spinning from lyotropic solutions (solutions that are rendered liquid crystalline by adding solvent molecules to liquid crystalline polymer) allows for high axial alignment of the liquid crystal molecules and thus affects the spinning performance, particularly if, as in the spider, there is a long region over which the fibre is drawn out by progressively increasing the linear flow rate of the dope. This also ensures molecular orientation throughout the fibre before the molecules are locked into position by a coagulation bath (in wet spinning) or in an air gap (in dry spinning). In fact, in order to realize the outstanding elastomeric properties of spider silk, the fibre's molecular rods and springs need to be well aligned; high-tenacity fibres such as Kevlar have, in contrast, very few in-built 'molecular springs' analogous to the spider's helices or  $\beta$ -turns, which explains the low elasticity of Kevlar. The absolute size of the molecules and their size distribution<sup>57</sup> are also important parameters affecting the toughness of the final thread: large variability in molecular size leads to incomplete molecular bonding. The toughness of spider dragline silk may thus depend in part on the fact that it contains predominantly a single large protein<sup>84,85</sup> with little variability in molecular weight<sup>2</sup>, achieved by the tight control inherent in nature's way of making proteins. Furthermore, the large molecular weight of this protein (~250 kDa) implies that the silk protein molecules cannot be fully extended in the dope; if they were, the material would turn into a gel at the high protein concentrations found in the storage sac and duct. In fact, molecules with a molecular weight over 30 kDa are difficult to spin industrially<sup>96</sup> because polymers with high molecular weight produce highly viscous spinning dopes. For example, the terephthalamides used for the production of DuPont's Kevlar and Acordis's Twaron have molecular weights of only 13–40 kDa, which is an order of magnitude smaller than that of spider silk proteins. These para-aramids, para-oriented aromatic nylons, are spun from concentrated solutions in concentrated sulphuric acid through a series of water baths, using highly controlled and narrow ranges of spinning rates and temperatures<sup>95</sup>. Clearly, spiders produce high quality fibres using a different method: they optimize dope viscosities and molecular conformations as well as spinneret design while keeping spinning conditions much more flexible<sup>63</sup>.

allow their efficient extrusion into a thread. An important lesson to learn from the spider is how it stores protein dope molecules in a highly concentrated liquid crystalline state and then extends these in the spinning duct to form a supremely tough thread. Learning this lesson may also help us to gain insight, through lateral thinking, into the sudden but unwanted assembly of other fibrous proteins, such as amyloids (the protein associated with Alzheimer's disease) that refold and form filaments where we had rather they did not. □

1. Fiber Economics Bureau. *Manufactured Fiber Review 2000*, Jan 2–53 (Fiber Economics Bureau, Washington, 1999).
2. O'Brien, J. P., Fahnestock, S. R., Termonia, Y. & Gardner, K. C. H. Nylons from nature: synthetic analogs to spider silk. *Adv. Mater.* **10**, 1185–1197 (1998).
3. Tirrell, J. G., Fournier, M. J., Mason, T. L. & Tirrell, D. A. Biomolecular materials. *Chem. Eng. News* **72**, 40–51 (1994).
4. Prince, J., McGrath, K., Digirolamo, C. & Kaplan, D. Construction, cloning, and expression of synthetic genes encoding spider dragline silk. *Biochemistry* **34**, 10879–10885 (1995).
5. Sun, Y., Shao, Z., Hu, P. & Tu, T. Hydrogen bonds in silk fibroin-poly(acrylonitrile-co-methyl acrylate) blends: FT-IR study. *J. Polym. Sci. B* **35**, 1405–1414 (1997).
6. Kaplan, D. L., Adams, W. W., Viney, C. & Farmer, B. L. (eds) *Silk Polymers: Materials Science and Biotechnology* 1–370 (ACS Books, Washington, 1994).
7. Shear, W. A., Palmer, J. M., Coddington, J. A. & Bonamo, P. M. A Devonian spinneret: early evidence of spiders and silk use. *Science* **246**, 479–481 (1989).

8. Selden, P. A. Orb-weaving spiders in the early Cretaceous. *Nature* **340**, 711 (1989).
9. Heslot, H. Artificial fibrous proteins: a review. *Biochimie* **80**, 19–31 (1998).
10. Asakura, T. & Kaplan, D. L. Silk production and processing. *Encyclop. Agric. Sci.* **4**, 1–11 (1994).
11. Kaplan, D., Adams, W. W., Farmer, B. & Viney, C. in *Silk Polymers. Materials Science and Biotechnology* (eds Kaplan, D., Adams, W. W., Farmer, B. & Viney, C.) 2–16 (American Chemical Society, Washington, 1994).
12. Seidel, A., Liivak, O. & Jelinski, L. W. Artificial spinning of spider silk. *Macromolecules* **31**, 6733–6736 (1998).
13. Vollrath, F. & Knight, D. P. Apparatus and method for forming materials. PCT Patent Application PCT/GB00/04489 (1999).
14. Kaplan, D. L. & Lombardi, S. J. The amino acid composition of major ampullate gland silk (Dragline) of *Nephila clavipes* (Araneae, Tetragnathidae). *J. Arachnol.* **18**, 297–306 (1990).
15. Winkler, S. & Kaplan, D. L. Molecular biology of spider silk. *Rev. Mol. Biotech.* **74**, 85–93 (2000).
16. Guerette, P., Ginzinger, D., Weber, B. & Gosline, J. Silk properties of determined by gland-specific expression of a spider fibroin gene family. *Science* **272**, 112–115 (1996).
17. Kovoov, J. La soie et les glandes sericigenes des arachnides. *Ann. Biol.* **16**, 97–171 (1977).
18. Kovoov, J. & Zylberberg, L. Fine structural aspects of silk secretion in a spider. *Tissue Cell* **14**, 519–530 (1982).
19. Kovoov, J. in *Ecophysiology of Spiders* (ed. Nentwig, W.) 160–186 (Springer, Berlin/Heidelberg/New York, 1987).
20. Vollrath, F., Wen Hu, X. & Knight, D. P. Silk production in a spider involves acid bath treatment. *Proc. R. Soc. B* **263**, 817–820 (1998).
21. Vollrath, F. & Knight, D. P. Structure and function of the silk production pathway in the spider *Nephila edulis*. *Int. J. Biol. Macromol.* **24**, 243–249 (1998).
22. Andersen, S. O. Amino acid composition of spider silks. *Comp. Biochem. Physiol.* **35**, 705–711 (1970).
23. Work, R. W. & Young, C. T. The amino acid compositions of major and minor ampullate silks of

- certain orb-web-building spiders (Araneae, Araneidae). *J. Arachnol.* **15**, 65–80 (1987).
24. Craig, C. L. Evolution of arthropod silks. *Annu. Rev. Entomol.* **42**, 231–267 (1997).
  25. Foelix, R. *Biology of Spiders* (Oxford Univ. Press, Oxford, 1996).
  26. Vollrath, F. in *Biomechanics in Animal Behaviour* (eds Domenici, P. & Blake, R. W.) 315–334 (Bios, Oxford, 2000).
  27. Vollrath, F. Spider webs and silk. *Sci. Am.* **266**, 70–76 (1992).
  28. Madsen, B., Shao, Z. & Vollrath, F. Variability in the mechanical properties of spider silks on three levels: interspecific, intraspecific and intraindividual. *Int. J. Biol. Macromol.* **24**, 301–306 (1999).
  29. Vollrath, F. Biology of spider silk. *Int. J. Biol. Macromol.* **24**, 81–88 (1999).
  30. Craig, C. L., Hsu, M., Kaplan, D. & Pierce, N. E. A comparison of the composition of silk proteins produced by spiders and insects. *Int. J. Biol. Macromol.* **24**, 109–118 (1999).
  31. Hayashi, C. Y. & Lewis, R. V. Evidence from flagelliform silk cDNA for the structural basis of elasticity and modular nature of spider silks. *Science* **287**, 1477–1479 (2000).
  32. Hinman, M., Dong, Z., Xu, M. & Lewis, R. W. Spider silk: a mystery starting to unravel. *Mater. Res. Soc. Symp.* **292**, 25–34 (1993).
  33. Hayashi, C. Y., Shipley, N. H. & Lewis, R. V. Hypotheses that correlate the sequence, structure and mechanical properties of spider silk proteins. *Int. J. Biol. Macromol.* **24**, 271–275 (1999).
  34. Kaplan, D. L., Prince, J. T., McGrath, K. P. & Digirolamo, C. M. Construction, cloning and expression of synthetic genes encoding spider dragline silk. *Biochemistry* **34**, 10879–10885 (1995).
  35. Gosline, J. M. et al. in *Silk Spiders. Materials Science and Biotechnology* (eds Kaplan, D., Adams, W. W., Farmer, B. & Viney, C.) 328–341 (American Chemical Society, Washington, 1994).
  36. Termonia, Y. Molecular modeling of spider silk elasticity. *Macromolecules* **27**, 7378–7381 (1994).
  37. Case, S. T. & Thornton, J. R. High molecular mass complexes of aquatic silk proteins. *Int. J. Biol. Macromol.* **24**, 89–101 (1999).
  38. Gosline, J., Denny, M. & DeMont, M. Spider silk as rubber. *Nature* **309**, 551–552 (1984).
  39. Simmons, A., Michal, C. & Jelinski, L. Molecular orientation and two-component nature of the crystalline fraction of spider dragline silk. *Science* **271**, 84–87 (1996).
  40. Kümmerlen, J., van Beek, J., Vollrath, F. & Meier, B. Local structure in spider dragline silk investigated by two-dimensional spin-diffusion nuclear magnetic resonance. *Macromolecules* **29**, 2920–2928 (1996).
  41. Frische, S., Maunsbach, A. B. & Vollrath, F. Elongate cavities and skin-core structure in *Nephila* spider silk observed by electron microscopy. *J. Microsc.* **189**, 64–70 (1998).
  42. Work, R. W. Duality in major ampullate silk and precursive material from orb-web-building spiders (Araneae). *Trans. Am. Microsc. Soc.* **103**, 113–121 (1984).
  43. Vollrath, F., Holtet, T., Thøgersen, H. & Frische, S. Structural organization of spider silk. *Proc. R. Soc. Lond. B* **263**, 147–151 (1996).
  44. Viney, C., Huber, A. E., Dunaway, D. L., Kerkam, K. & Case, S. T. in *Silk Polymers. Materials Science and Biotechnology* (eds Kaplan, D., Adams, W. W., Farmer, B. & Viney, C.) 120–136 (American Chemical Society, Washington, 1994).
  45. Mahoney, D. V., Vezie, D. L., Eby, R. K., Adams, W. W. & Kaplan, D. in *Silk Polymers. Materials Science and Biotechnology* (eds Kaplan, D., Adams, W. W., Farmer, B. & Viney, C.) 196–210 (American Chemical Society, Washington, 1994).
  46. Shao, Z., Wen Hu, X., Frische, S. & Vollrath, F. Heterogeneous morphology in *Nephila edulis* spider silk and its significance for mechanical properties. *Polymers* **40**, 4709–4711 (1999).
  47. Hijirida, D. H., Do, K. G., Michal, C., Wong, S., Zax, D. & Jelinski, L. W. C13 NMR of *Nephila clavipes* major ampullate silk gland. *Biophys. J.* **71**, 3442–3447 (1996).
  48. Akai, H. The structure and ultrastructure of the silk gland. *Experientia* **39**, 443–449 (1983).
  49. Knight, D. P. & Vollrath, F. Liquid crystals and flow elongation in a spider's silk production line. *Proc. R. Soc. Lond. B* **266**, 519–523 (1999).
  50. Weiskopf, A., Senecal, K., Vouros, P., Kaplan, D. & Mello, C. M. The carbohydrate composition of spider silk: *Nephila edulis* dragline. *Glycobiology* **6**, 1703 (1996).
  51. Vollrath, F. & Tillinghast, E. K. Glycoprotein glue beneath a spiders web's aqueous coat. *Naturwissenschaften* **78**, 557–559 (1991).
  52. Kerkam, K., Viney, C., Kaplan, D. & Lombardi, S. Liquid crystallinity of natural silk secretions. *Nature* **349**, 596–598 (1991).
  53. Willcox, P. J., Gido, S. P., Müller, W. & Kaplan, D. L. Evidence of a cholesteric liquid crystalline phase in natural silk spinning processes. *Macromolecules* **29**, 5106–5110 (1996).
  54. Magoshi, J., Magoshi, Y. & Nakamura, S. Crystallization, liquid crystal, and fiber formation of silk fibroin. *J. Appl. Polym. Sci.* **41**, 187–204 (1985).
  55. Nakamae, K., Nishino, T. & Ohkubo, H. Elastic modulus of the crystalline regions of silk fibroin. *Polymer* **30**, 1243–1246 (1989).
  56. Bunning, J. D. & Lydon, J. E. The cellular optical texture of the lyotropic nematic phase of the caesium pentadecafluoro-octanoate (ScPFO) water system in cylindrical tubes. *Liquid Cryst.* **20**, 381–385 (1996).
  57. Donald, A. M. & Windle, A. H. *Liquid Crystalline Polymers* 1–310 (Cambridge Univ. Press, Cambridge, 1992).
  58. Northolt, M. G. & Sikkema, D. J. Lyotropic main chain liquid crystal polymers. *Adv. Polym. Sci.* **98**, 115–177 (1991).
  59. Knight, D. P., Knight, M. M. & Vollrath, F. Beta transition and stress-induced phase separation in the spinning of spider dragline silk. *Int. J. Biol. Macromol.* **27**, 205–210 (2000).
  60. Riekel, C., Madsen, B., Knight, D. & Vollrath, F. Single fibre X-ray diffraction of spider silk. *Biol. Macromol.* (in the press).
  61. Palmer, J., Coyle, F. & Harrison, F. Structure and cyto-chemistry of the silk glands of the mygalomorph spider *Antrodiaetus unicolor* (Aranea, Antrodiaetidae). *J. Morphol.* **174**, 269–274 (1982).
  62. Tillinghast, E., Chase, S. & Townley, M. Water extraction by the major ampullate duct during silk formation in the spider, *Argiope aurantia* Lucas. *J. Insect Physiol.* **30**, 591–596 (1984).
  63. Vollrath, F., Madsen, B. & Shao, Z. The effect of spinning conditions on the mechanical properties of a spider's dragline. *Proc. R. Soc. Lond.* (in the press).
  64. Shultz, J. W. The origin of the spinning apparatus in spiders. *Biol. Rev.* **62**, 89–113 (1987).
  65. Tillinghast, E. K., Townley, M. A., Bernstein, D. T. & Gallagher, K. S. Comparative study of orb web hygroscopicity and adhesive spiral composition in three araneid spiders. *J. Exp. Zool.* **259**, 154–165 (1991).
  66. Schildknecht, H., Munzelmann, P., Krauss, D. & Kuhn, C. Über die chemie der spinnwebe. *Naturwissenschaften* **59**, 98–99 (1972).
  67. Vollrath, F. et al. Compounds in the droplets of the orb spider's viscid spiral. *Nature* **345**, 526–528 (1990).
  68. Edmonds, D. & Vollrath, F. The contribution of atmospheric water vapour to the formation and efficiency of a spider's web. *Proc. R. Soc. Lond.* **248**, 145–148 (1992).
  69. Vollrath, F. & Edmonds, D. Modulation of the mechanical properties of spider silk coating with water. *Nature* **340**, 305–307 (1989).
  70. Peters, H. M. Über den Spinnapparat von *Nephila madagascariensis* (Radnetzspinnen Argioidae). *Z. Naturforsch.* **10**, 395–404 (1955).
  71. Knight, D. P. & Vollrath, F. Changes in element composition along the spinning duct in a *Nephila* spider. *Naturwissenschaften* (in the press).
  72. Gosline, J. M., DeMont, M. E. & Denny, M. W. The structure and properties of spider silk. *Endeavour* **10**, 31–43 (1986).
  73. Vincent, J. F. V. *Structural Materials* 1–378 (Macmillan, London, 1982).
  74. Shao, Z. & Vollrath, F. The effect of solvents on the contraction and mechanical properties of spider silk. *Polymer* **40**, 1799–1806 (1999).
  75. Magoshi, J., Magoshi, Y. & Nakamura, S. Physical properties and structure of silk: 10. The mechanism of fibre formation from liquid silk of silkworm *Bombyx mori*. *Polym. Comm.* **26**, 309–311 (1985).
  76. Gamo, T. Genetic variants of the *Bombyx mori* silkworm encoding sericin proteins of different lengths. *Biochem. Genet.* **20**, 165–177 (1982).
  77. Sehnal, F. & Akai, H. Insect silk glands—their types, development and function, and effects of environmental-factors and morphogenetic hormones on them. *Int. J. Insect Morphol.* **19**, 79–132 (1990).
  78. Hepburn, H. R., Kurstjens, S. P. The combs of honeybees as composite-materials. *Apidologie* **19**, 25–36 (1988).
  79. Hendersen, G., Manweiler, S. A., Lawrence, W. J., Tempelman, R. J. & Foil, L. D. The effects of *Steinernema capocapsae* (Weiser) application to different life stages on adult emergence of the cat flea *Ctenocephalides felis* (Bouche). *Vet. Dermatol.* **6**, 159–163 (1995).
  80. Zemlin, J. C. A Study Of The Mechanical Behavior Of Spider Silks 1–38 (Clothing and Organic Materials Laboratory Report, US Army Natick Labs, Natick, 1968).
  81. Engstler, M. S. Studies on silk secretion in the Trichoptera (F. Limnephilidae). *Cell Tissue Res.* **169**, 77–92 (1976).
  82. Sivinski, J. Prey attraction by luminous larvae of the fungus gnat *Orfelia fultoni*. *Ecol. Entomol.* **7**, 443–446 (1982).
  83. Hunt, S. Amino acid composition of silk from the pseudoscorpion *Neobisium maritimum* (Leach): a possible link between the silk fibroins and the keratins. *Comp. Biochem. Physiol.* **34**, 773–777 (1970).
  84. Winkler, S. & Kaplan, D. L. Molecular biology of spider silk. *Rev. Mol. Biotech.* (in the press).
  85. Mello, C. M., Senecal, K., Yeung, B., Vouros, P. & Kaplan, D. in *Silk Polymers. Materials Science and Biotechnology* (eds Kaplan, D., Wade, W. W., Farmer, B. & Viney, C.) 67–79 (American Chemical Society, Washington, 1994).
  86. Candelas, G., Candelas, T., Ortiz, A. & Rodriguez, O. Translational pauses during a spider fibroin synthesis. *Biochem. Biophys. Res. Commun.* **116**, 1033–1038 (1983).
  87. van Raaij, M. J., Mitraki, A., Lavigne, G. & Cusack, S. A triple beta-spiral in the adenovirus fibre shaft reveals a new structural motif for a fibrous protein. *Nature* **401**, 935–938 (1999).
  88. van Beek, J. D., Kümmerlen, D., Vollrath, F. & Meier, B. H. Supercontracted spider dragline silk: a solid-state NMR study of the local structure. *Int. J. Biol. Macromol.* **24**, 173–178 (1999).
  89. Yeh, W.-Y. & Young, R. J. Molecular deformation processes in aromatic high modulus polymer fibres. *Polymer* **40**, 857–870 (1999).
  90. Shao, Z., Young, R. J. & Vollrath, F. The effects of solvents on spider silk studied by mechanical testing and single-fibre Raman spectroscopy. *Int. J. Biol. Macromol.* **24**, 295–300 (1999).
  91. Sirichaisit, S., Young, R. J. & Vollrath, F. Molecular deformation in spider dragline silk subjected to stress. *Polymers* **41**, 1223–1227 (1999).
  92. Riekel, C. et al. Aspects of x-ray diffraction on single spider fibers. *Macromolecule* **24**, 179–186 (1999).
  93. Grubb, D. T. & Jelinski, J. W. Fiber morphology of spider silk: the effects of tensile deformation. *Macromolecule* **30**, 2860–2867 (1997).
  94. Fung, Y. C. *Biomechanics* 1–586 (Springer, Heidelberg, 1981).
  95. Askeland, D. R. *The Science and Engineering of Materials* (PWS, Boston, 1994).
  96. Yoon, H. N., Charbonneau, L. F. & Calundann, G. W. Synthesis, processing and properties of thermotropic liquid-crystal polymers. *Adv. Materials* **4**, 206–214 (1992).
  97. Thiel, B. & Viney, C. A nonperiodic lattice model for crystals in *Nephila clavipes* major ampullate silk. *Mater. Res. Bull.* **20**, 52–56 (1995).

Acknowledgements

We thank B. Meier, R. Young, S. Case, J. Kenney, D. LaFollette, C. Craig, D. Kaplan, J. Gosline and H. Coulsey for their perceptive and helpful comments. Our research on spider silk has been funded by the Danish Science Research Council (SNF), the Science Faculty of Aarhus University, the Carlsberg Foundation, the Danish Academic Exchange Programme, the US Army (RDSG), the British Biological and Engineering Research Councils (BBSRC, EPSRC), the European Synchrotron Radiation Facility (ESRF) and the European Science Foundation (ESF). F.V. thanks the director and staff of Mpala Research Centre for their hospitality; D.P.K. thanks the Biological Imaging Centre at Southampton University for technical assistance and we both are grateful to our many collaborators for their help and support.

Correspondence and requests for materials should be addressed to F.V. (e-mail: fritz.vollrath@zoo.ox.ac.uk).